Metrologia

PAPER

Comparison of Open and Solid Falling Retroreflector Gravimeters*

IOP Publishing Metrologia

Metrologia **57** (2020) 035012 (8pp) https://doi.org/10.1088/1681-7575/ab7d12

Comparison of Open and Solid Falling Retroreflector Gravimeters

Neil Ashby[1,2] **and Derek van Westrum**[3]

[1] Associate, Physical Measurement Laboratory, National Institute of Standards and Technology, Boulder, CO 80305, United States of America
[2] Department of Physics, University of Colorado, Boulder, CO 80309, United States of America
[3] National Geodetic Survey, Boulder, CO, United States of America

E-mail: ashby@boulder.nist.gov

Received 2 January 2020, revised 3 March 2020
Accepted for publication 5 March 2020
Published 29 May 2020

Abstract

We study whether the optical properties of a solid glass retroreflector influence the value of the acceleration of gravity g determined by dropping both solid and open retroreflectors in an absolute ballistic gravimeter. The retroreflectors have equivalent optical centers and are dropped from the same height, at a fixed location, in the same gravimeter while recording time data corresponding to fixed fringe separation intervals of 400 fringes. The data for both types of retroreflectors are processed with commercial software, as well as with independently developed software based on a relativistic treatment of the phase difference between reference beam and test beams, and a realistic treatment of the effect of frequency modulation, with modulation index $\beta \gg 1$, on the interference signal. After applying corrections for polar motion, barometric admittance, tides, and ocean loading we find agreement between the values of g determined with both types of retroreflectors, whether processed with commercial software or with our independently developed software. We suggest two procedures for computing relativistic corrections; the two methods agree to better than 0.01 μGal.

Keywords: gravimeters, relativity, acceleration, retroreflectors

(Some figures may appear in colour only in the online journal)

1. Introduction

In an absolute falling retroreflector gravimeter, a reference laser beam is partially reflected upwards from a stationary beamsplitter and then back down from a falling retroreflector (a 'cube'). Counting interference fringes between the reference and test beams may then be used to measure the local acceleration of gravity, g. In a previous work [1], the beams were assumed to combine at the beamsplitter; relativistic considerations led to the following expression for the interference signal at $Z = 0$ ([1], equation (33)):

$$\phi(t) = \frac{2(Dn-d)\Omega}{c} + \frac{2\Omega Z_0}{c} - \frac{2(Dn-d)\Omega V_0}{c^2} - \frac{2\Omega Z_0 V_0}{c^2} + t\left(-\Omega + \frac{2\Omega V_0}{c} - \frac{2\Omega V_0^2}{c^2} + \frac{2\Omega g(Dn-d)}{c^2} + \frac{2\,g\Omega Z_0}{c^2}\right) + t^2\left(-\frac{g\Omega}{c} + \frac{3\,g\Omega V_0}{c^2}\right)) - \frac{g^2\Omega t^3}{c^2} + \gamma\Omega\left(t(-\frac{2(Dn-d)Z_0}{c^2} - \frac{2Z_0^2}{c^2}) + t^2(\frac{Z_0}{c} - \frac{(Dn-d)V_0}{c^2} - \frac{4V_0Z_0}{c^2}) + t^3(\frac{V_0}{3c} + \frac{g(Dn-d)}{3c^2} - \frac{4V_0^2}{3c^2} + \frac{7\,gZ_0}{3c^2}) + t^4(-\frac{g}{12c} + \frac{5\,gV_0}{4c^2}) - \frac{g^2t^5}{4c^2}\right) \quad (1)$$

where c is the speed of light, Ω is angular frequency of the light, D is the face-to-corner distance of the retroreflector (the "cube"), d is the distance from face to center of mass, n is the index of refraction, Z_0 and V_0 are the position and velocity of the cube at the initial time $T = 0$, g is the acceleration of

[4] This paper is a contribution of the U. S. government and is not subject to copyright. The use of commercial products does not imply endorsement by NOAA or NIST.

gravity at the beamsplitter and γ is the gravity gradient. The origin of coordinates is at the beamsplitter and the coordinate Z is positive upwards.

This expression is the basis for the present study. The apparently large effect on g arising from dimensions and refractive index of the cube resulted in several critical comments [2–4], and replies [5–7], without throwing light on the real issues. D'Agostino [8] simulated dropping of glass and open retroreflectors using only the difference $\phi(t)-\phi(0)$ for the interference observations. This subtraction removes non-relativistic terms responsible for the predicted change [1] in g, as well as some relativistic contributions. The simulated results approximately agree with the results reported in the present paper for reasons discussed below; however we do not neglect relativistic contributions to the phase.

There are two problems with the literal application of an interference signal that is produced at the beamsplitter. The first is that in some gravimeters the reference beam, or the test beam, or both, are transported unequal distances by fibers and/or mirrors before interference takes place [9]; this introduces an unknown constant phase between the reference and test beams. Also, the interference signal occurs within the argument of a trigonometric function–such as a cosine–and is undetermined to within a constant added integral multiple of 2π. This issue is treated in detail in section 3, where a theory of frequency modulation by a signal with modulation index β that is large compared to unity is developed. These facts lead to reconsideration of the choice of fit parameters and the effect on g of the cube's properties.

In the following section, we discuss the choice of fit parameters, and the effect on g. The constant parameter combination Z_0+Dn-d disappears from the non-relativistic part of the phase and becomes a small relativistic contribution. Two methods are presented in section 4 for explicitly computing relativistic effects arising from the cube's velocity. Measurements made at Table Mountain, Boulder, CO, with open and solid cubes of comparable dimensions, in similar dropping chambers, are described and discussed in section 4.1; to within measurement uncertainties the same value of g was obtained–at the same location and during comparable time periods. The relativistic corrections–obtained in two ways–were in agreement to within 0.01 μGal[5]. Sections 5 and 6 compare the data analysis using commercial software and software based on the present theory, respectively.

2. The parameter Z_0

Four constant parameters are usually used to describe the falling cube: The initial position Z_0, initial velocity V_0, and the acceleration of gravity g and its gradient γ at the chosen origin of coordinates, which in [1] was the point of separation and recombination of the beams, at the beamsplitter. The interference phase at the beamsplitter was calculated neglecting quadratic and higher order terms in the gravity gradient γ and to this order may be compactly expressed as

$$\phi(t)=\Omega F(t)=-\frac{2\Omega}{c}(Z_{\rm cm}(t)+Dn-d)\left(1-\frac{V_{\rm cm}(t)}{c}\right). \quad (2)$$

$F(t)$ is independent of frequency, and can be separated into non-relativistic and relativistic parts:

$$F(t)=\frac{1}{c}F_{nr}(t)+\frac{1}{c^2}F_{\rm rel}(t)\,. \quad (3)$$

$Z_{\rm cm}(t)$ and $V_{\rm cm}(t)$ are the center of mass (CM) position and velocity, given by

$$Z_{\rm cm}(t)=Z_0+V_0t-\frac{gt^2}{2}+\gamma\left(\frac{Z_0t^2}{2}+\frac{V_0t^3}{6}-\frac{gt^4}{24}\right); \quad (4)$$

$$V_{\rm cm}(t)=V_0-gt+\gamma\left(Z_0t+\frac{V_0t^2}{2}-\frac{gt^3}{6}\right). \quad (5)$$

Equation (2) is mathematically equivalent, to first order in γ, to the interference phase, equation(1), and allows one to cleanly separate relativistic from non-relativistic contributions. The purpose of this section is to show that, contrary to many statements in the literature, Z_0 cannot always be considered a useful parameter in data fitting. To make this clearer, in the remainder of this section we discuss a non-relativistic model, without the complication of relativistic effects.

Assuming there is no modulation, the phase of the interference signal at the beamsplitter where recombination was assumed to occur is

$$\phi(t)=-\frac{2\Omega}{c}\left(Z_0+Dn-d+V_0t-\frac{1}{2}gt^2+\gamma(\frac{1}{2}Z_0t^2+\frac{1}{6}V_0t^3-\frac{1}{24}gt^4)\right)\times\left(1-\frac{V_{\rm cm}(t)}{c}\right) \quad (6)$$

The non-relativistic form of this limiting phase is obtained by making the replacement

$$\Omega\to\frac{2\pi c}{\lambda}. \quad (7)$$

Then in the non-relativistic approximation,

$$\phi(t)=-\frac{4\pi}{\lambda}\left(Z_0+Dn-d+V_0t-\frac{1}{2}gt^2+\gamma(\frac{1}{2}Z_0t^2+\frac{1}{6}V_0t^3-\frac{1}{24}gt^4)\right). \quad (8)$$

A minus sign was introduced so that the coefficient of the term in gt^2 is positive, corresponding to measurements in which the number of fringes increases with time. This phase occurs in the argument of a cosine function, to which an arbitrary multiple of 2π can be added without changing the cosine's magnitude; this is discussed in detail in section 3. The observable phase is equivalent to

$$\phi(t)+2\pi M, \quad (9)$$

[5] 1 μGal $=10^{-8}$ m s^{-2}.

where M is an unknown, arbitrary integer. Any constant contribution on the right side of equation (8) can be combined with the term $2\pi M$ leaving a residual phase ψ:

$$2\pi M - \frac{4\pi}{\lambda}(Z_0 + Dn - d) = \psi\,. \tag{10}$$

The observable phase in a non-relativistic approximation is therefore

$$\phi(t) = \psi - \frac{4\pi}{\lambda}\left(V_0 t - \frac{1}{2}gt^2 + \gamma(\frac{1}{2}Z_0 t^2 + \frac{1}{6}V_0 t^3 - \frac{1}{24}gt^4)\right). \tag{11}$$

The terms $Dn - d$ contribute instead to the relativistic part of the phase. The parameter Z_0 now contributes only weakly, since it is multiplied by the gradient γ. The phase in equation (11) suggests fitting the data (neglecting relativistic effects) using the parameters $\{\psi, Z_0, V_0, g\}$. The results are not reliable because both g and Z_0 have coefficients proportional to t^2: g and Z_0 are highly correlated and the covariance matrix is nearly singular. Inclusion of relativistic terms does not improve the situation. The difficulty may be remedied by combining g and Z_0 into a single parameter. Let

$$g_t = g - \gamma Z_0\,. \tag{12}$$

We also replace g in the last term of equation (11) by g_t. At a maximum drop time of 0.3 s., with $Z_0 \approx 0.75$ m the error of the latter replacement is of order

$$\frac{\pi}{6\lambda}\gamma^2 Z_0 t^4 \approx 5\times 10^{-7} \text{ radians}, \tag{13}$$

which is negligible as it cannot give rise to a significant number of fringes. Then Z_0 disappears from the non-relativistic model. The fit parameters become ψ, V_0, g_t. In this scheme the covariance matrix is non-singular. Relativistic contributions depend on the velocity of the center of mass, which can also be written to the same order in terms of g_t:

$$\begin{aligned} V_{\rm cm}(t) &= V_0 - gt + \gamma(Z_0 t + \frac{1}{2}V_0 t^2 - \frac{1}{6}gt^3) \\ &\approx V_0 - g_t t + \gamma(\frac{1}{2}V_0 t^2 - \frac{1}{6}g_t t^3) \end{aligned} \tag{14}$$

The phase error introduced by the quadratic term in γ is less than 10^{-20} radians. However the value of g_t at the 'top of the drop' is no longer at a fixed location in the chosen coordinate system, but includes variations in initial drop position, thus might suffer from greater errors than if it were evaluated at a fixed location in the coordinate system. This is consistent with some previously published models (see e.g. appendix of [9]), in which the acceleration of the cube is written as

$$\ddot{Z} = -g + \gamma(Z - Z_0)\,. \tag{15}$$

Here g would be evaluated for a particular drop at the initial instant when $Z = Z_0$ and might vary depending on the consistency of release.

3. Modulation; choice of fit parameters

The purpose of this section is to develop an appropriate expression for the frequency-modulated interference signal with large modulation index, including relativistic effects. This is based on the interference phase in equation (2). If the reference signal is modulated at angular frequency ω with amplitude ω_m, the instantaneous angular frequency can be written $\Omega + \omega_m \cos(\omega t + \phi)$. Then apart from a constant of integration, the signal phase will be

$$\int^t \big(\Omega + \omega_m \cos(\omega t + \phi)\big)dt = \Omega t + \beta \sin(\omega t + \phi) \tag{16}$$

where $\beta = \omega_m/\omega$ is the modulation index. In the gravimeter used in the present experiment, the laser light is modulated at $\omega = (2\pi)\times$ 8333 Hz with peak-to-peak amplitude 6 MHz [13], so

$$\beta \approx \frac{3\times 10^6}{8333} = 340 \gg 1\,. \tag{17}$$

An expansion for small modulation index is inappropriate. Let the reference beam emerging from the beam splitter be represented by the scalar wavefunction

$$\Psi_{\rm ref} = e^{-i\Omega t - i\beta\sin(\omega t + \phi)} \tag{18}$$

where $\beta\sin(\phi)$ represents the phase difference between the reference beam and the modulation at time $t = 0$.

Thus, in addition to the principal frequency Ω, frequencies $\Omega \pm n\omega$ will be present, where n can be any integer. For a signal of frequency Ω', equation (2) shows that the final phase of the signal that passes up through the retroreflector and back to the beamsplitter is proportional to Ω', so that at the beamsplitter the component of frequency Ω becomes

$$e^{-i\Omega t} \to e^{-i\Omega(t + F(t))}; \tag{19}$$

and for the side frequency terms,

$$e^{-i\Omega t \pm in\omega t} \to e^{(-i\Omega \pm in\omega)(t + F(t))}. \tag{20}$$

The function $F(t)$ was defined in equation (3). The test beam is therefore

$$\Psi_{\rm test} = e^{-i\Omega(t + F(t)) + \beta\sin(\omega t + \omega F(t) + \phi)}\,. \tag{21}$$

We assume the wavefunctions are superimposed at the beamsplitter with equal amplitudes, so the net signal is

$$\Psi = \Psi_{\rm ref} + \Psi_{\rm test}\,. \tag{22}$$

The intensity of the signal will be proportional to

$$\begin{aligned} |\Psi|^2 &= |\Psi_{\rm ref}|^2 + |\Psi_{\rm test}|^2 + \Psi_{\rm ref}\Psi^*_{\rm test} + \Psi^*_{\rm ref}\Psi_{\rm test} \\ &= 2 + 2\cos(\Omega F(t) + \beta\big(\sin(\omega t + \phi + \omega F(t)) - \sin(\omega t + \phi)\big) \\ &= 2 + 2\cos(\Omega F(t) + \beta\big(\sin(\omega t + \phi)(\cos(\omega F(t)) - 1) \\ &\quad + \cos(\omega t + \phi)\sin(\omega F(t))\big)\,. \end{aligned} \tag{23}$$

In the present experiment, for each drop 2700 times were recorded separated by 400 fringes, so the maximum value of the function $F(t)$ can be estimated by setting

$$F(t_{\max})\Omega = (2\pi)\times 400\times 2700, \quad \text{or} \quad F_{\max} = 2.85\times 10^{-9}\text{s}; \tag{24}$$

then $\omega F_{\max} \approx 0.000\,15 \ll 1$. Even with β as large as it is, we can make the approximations

$$\cos(\omega F(t)) \approx 1, \quad \sin(\omega F(t)) \approx \omega F(t)\,. \tag{25}$$

The signal intensity then simplifies to

$$|\Psi|^2 = 2 + 2\cos(\Omega F(t) + \beta\omega F(t)\cos(\omega t + \phi))\,. \tag{26}$$

The function $F(t)$ is given in equation (3) as the sum of non-relativistic and relativistic contributions:

$$F_{nr}(t) = -2(Z_{\rm cm}(t) + Dn - d); \quad F_{\rm rel} = 2V_{\rm cm}(t)(Z_{\rm cm}(t) + Dn - d)\,. \tag{27}$$

One factor $1/c$ is cancelled out when the replacement $\Omega \to (2\pi c/\lambda)$ is made. The number of fringes counted $N(t)$ will be determined by the argument of the interference cosine, which is

$$N_{total} = \frac{1}{2\pi}\left(\Omega F(t) + \beta\big(\cos(\omega t + \phi)\omega F(t)\big)\right). \tag{28}$$

The phase is undetermined to within an added integral multiple of 2π:

$$\begin{aligned} N(t) &= \frac{1}{2\pi}\big(2\pi M + \Omega F(t) + \beta\cos(\omega t + \phi)\omega F(t)\big) \\ &= M + \frac{1}{2\pi}\left(\frac{2\pi c}{\lambda}\left(\frac{1}{c}F_{nr} + \frac{1}{c^2}F_{\rm rel}\right) + \beta\omega(\cos(\phi)\cos(\omega t)\right. \\ &\quad \left. - \sin(\phi)\sin(\omega t))\left(\frac{1}{c}F_{nr} + \frac{1}{c^2}F_{\rm rel}\right)\right) \\ &= M + \frac{1}{\lambda}\big(1 + \lambda A\cos(\omega t) + \lambda B\sin(\omega t)\big)\left(F_{nr} + \frac{1}{c}F_{\rm rel}\right), \end{aligned} \tag{29}$$

where M is an unknown integer and

$$A\cos(\omega t) + B\sin(\omega t) = \frac{\beta\omega}{2\pi c}\cos(\omega t + \phi)\,. \tag{30}$$

Thus the modulation index is related to the amplitudes A and B by

$$\sqrt{A^2 + B^2} = \frac{\beta\omega}{2\pi c}; \tag{31}$$

although the modulation index is large, the coefficients A and B will be small. Apart from the arbitrary whole number M, The nonrelativistic fringe function is then

$$N_{nr}(t) = -2\left(\frac{1}{\lambda} + \big(A\cos(\omega t) + B\sin(\omega t)\big)\right)(Z_{\rm cm}(t) + dn - d) \tag{32}$$

and the relativistic contributions, showing explicitly the factor c^{-1}, are

$$\begin{aligned} N_{\rm rel}(t) = N(t) - N_{nr}(t) = \frac{1}{c\lambda}F_{\rm rel}(t) + \frac{1}{c}\big(A\cos(\omega t) \\ + B\sin(\omega t)\big)F_{\rm rel}(t)\,. \end{aligned} \tag{33}$$

The functions F_{nr} and $F_{\rm rel}$ are given by

$$F_{nr} + \frac{1}{c}F_{\rm rel} = -2\big(Z_{\rm cm}(t) + Dn - d\big)\left(1 - \frac{V_{\rm cm}(t)}{c}\right). \tag{34}$$

If $\omega F(t)$, which is slowly varying, were treated as a constant then we would simply have the two parameters A and B to add to the list of parameters to be fit. Including two such constant parameters typically reduces the residuals by a factor of 5 or more without having much impact on g. Including the variation due to $F(t)$ results in reduction in the residuals by roughly 3% to 4% for this experiment. As discussed in the previous section, writing the CM position and velocity in terms of g_t, eliminates Z_0 from the model. Consider the non-relativistic contributions to the fringe number in equation (32) at $t = 0$, where we regard the arbitrary M as part of the non-relativistic contribution. (Our approach is to group the relativistic constant contributions with the relativistic corrections.)

$$N_{nr}(0) = M + \frac{1}{\lambda}(1 + \lambda A)(Z_0 + Dn - d)\,. \tag{35}$$

We replace these constant contributions by a residual phase constant $\frac{\psi}{2\pi}$, so the number of observed fringes becomes

$$\begin{aligned} N(t) = \frac{\psi}{2\pi} - \frac{1}{\lambda}(1 + \lambda A)(Z_0 + Dn - d) \\ + \frac{1}{\lambda}\big(1 + \lambda A\cos(\omega t) + \lambda B\sin(\omega t)\big)\left(F_{nr} + \frac{1}{c}F_{\rm rel}\right), \end{aligned} \tag{36}$$

As discussed in section 2, introducing g_t as in equation (12) and making the approximation $g \to g_t$ removes the parameter Z_0 from the model. The parameters to be fit are ψ, V_0, g_t, A, B. We discuss fitting data obtained with both open and solid retroreflectors using this model in sections 5 and 6.

4. Relativistic corrections

Fitting a theoretical expression for fringe number $N(t_j)$ that depends on a set of fit parameters p_k involves the covariance matrix

$$C_{kl} = \sum_j \frac{\partial N(t_j)}{\partial p_k}\frac{\partial N(t_j)}{\partial p_l}\,, \tag{37}$$

where the recorded times are t_j at epoch j and where the measured total number of fringes is $M_j = M(t_j)$. Guessing values $p_k^{(0)}$ for the fit parameters, and substituting these into the $N(t_j)$ and its partial derivatives, the next approximation will be

$$p_k^{(1)} = p_k^{(0)} + \sum_l \big(C^{-1}\big)_{kl}\sum_j (M_j - N(t_j))\frac{\partial N(t_j)}{\partial p_l}\,. \tag{38}$$

The improved parameter values $p_k^{(1)}$ are substituted into the right side of equation (38) and the process is repeated until there is no further change in any parameter. At this point the covariance matrix is non-singular so the residuals satisfy

$$\sum_j (M_j - N(t_j)) \frac{\partial N(t_j)}{\partial p_l} = 0\,. \tag{39}$$

Equation (39) permits the development of an explicit expression for the relativistic contribution to the determination of g. Divide the theoretical expression for the fringe number into non-relativistic and relativistic contributions; the latter will be of order c^{-1}, where c is the speed of light. Only first order terms in an expansion in powers of c^{-1} need be kept. Then

$$N(t_j) = N_{nr}(t_j) + N_{\rm rel}(t_j), \tag{40}$$

and the covariance matrix becomes

$$C_{kl} = \sum_j \frac{\partial N_{nr}}{\partial p_k}\frac{\partial N_{nr}}{\partial p_l} + \sum_j \left(\frac{\partial N_{nr}}{\partial p_k}\frac{\partial N_{\rm rel}}{\partial p_l} + \frac{\partial N_{\rm rel}}{\partial p_k}\frac{\partial N_{nr}}{\partial p_l} \right) \tag{41}$$

$$= C_{kl}^{nr} + C_{kl}^{rel}\,, \tag{42}$$

where to simplify the notation the arguments t_j have been suppressed. The inverse covariance matrix can be expanded in powers of C^{-1}:

$$C^{-1} = (C^{nr})^{-1} - (C^{nr})^{-1} C^{rel} (C^{nr})^{-1}\,. \tag{43}$$

Then equation (38) becomes approximately

$$\begin{aligned} p_k^{(1)} = p_k^{(0)} &+ \sum_l (C^{nr})_{kl}^{-1} \sum_j (M_j - N_{nr}(t_j)) \frac{\partial N_{nr}(t_j)}{\partial p_l} \\ &+ \sum_l \left((C^{nr})^{-1} C^{rel} (C^{nr})^{-1} \right)_{kl} \sum_j (M_j - N_{nr}(t_j)) \\ &\times \frac{\partial N_{nr}(t_j)}{\partial p_l} + \sum_l (C^{nr})_{kl}^{-1} \sum_j (M_j - N_{nr}(t_j)) \frac{\partial N_{\rm rel}(t_j)}{\partial p_l} \\ &- \sum_l (C^{nr})_{kl}^{-1} \sum_j N_{\rm rel}(t_j) \frac{\partial N_{nr}(t_j)}{\partial p_l}\,. \end{aligned} \tag{44}$$

Then one can consider the following approximate iteration scheme. First neglect the last three lines of equation (44), fitting the parameters using only the non-relativistic theory expressed in the first line. The non-relativistic values of these parameters can then be inserted into the remaining terms in lines 2 through 4 since each of these terms already contains a factor c^{-1}. But the iteration process has converged and reduces the first line,

$$\sum_l (C^{nr})_{kl}^{-1} \sum_j (M_j - N_{nr}(t_j)) \frac{\partial N_{nr}(t_j)}{\partial p_l}$$

to a negligible level. Then line 2 is also negligible. Line 3 is not identically zero but is found to be negligibly small because each term $M_j - N_{nr}(t_j)$ is small, a result of the fit. The relativistic contributions to the parameters are then simply:

$$p_k^{rel} = -\sum_l (C^{nr})_{kl}^{-1} \sum_j N_{\rm rel}(t_j) \frac{\partial N_{nr}(t_j)}{\partial p_l}\,. \tag{45}$$

One may check equation (45) by first fitting the parameters using equation (38) with the complete expression for $N(t_j)$, instead of N_{nr}, and then subtracting the non-relativistic fit obtained from iterating the non-relativistic model:

$$(p_k^{nr})^{(1)} = (p_k^{nr})^{(0)} + \sum_l \left((C^{nr})^{-1} \right)_{kl} \sum_j (M_j - N_{nr}(t_j)) \frac{\partial Nnr(t_j)}{\partial p_l}\,. \tag{46}$$

The relativistic corrections, equation (45), were found to agree within 0.01 μGal with the differences in the fits with open and solid retroreflectors reported in tables 1 through 4.

4.1. Correcting recorded times for relativity.

Another approach is to model the fringe count non-relativistically, as in equation (32), but seek corrections δt to the recorded times, such that correcting the time data brings the data into agreement with the full relativistic model. The nonrelativistic fringe function can be written:

$$N_{nr}(t) = -\frac{2}{\lambda}\left(Z_{\rm cm}(t) + Dn - d\right)\left(1 + \frac{\beta\omega\lambda}{2\pi c}\cos(\omega t + \phi)\right), \tag{47}$$

and the relativistic contribution to the fringe function, from equations (33) and (34) is

$$N_{\rm rel} = \frac{2V_{\rm cm}(t)}{\lambda c}\left(Z_{\rm cm}(t) + Dn - d\right)\left(1 + \frac{\beta\omega\lambda}{2\pi c}\cos(\omega t + \phi)\right). \tag{48}$$

We replace t by $t + \delta t$ in equation (47) and expand to first order:

$$\begin{aligned} N_{nr}(t+\delta t) &= N_{nr}(t) + \frac{dN_{nr}(t)}{dt}\delta t \\ &= N_{nr}(t) - \frac{2}{\lambda}V_{\rm cm}(t)\left(1 + \frac{\beta\omega\lambda}{2\pi c}\cos(\omega t + \phi)\right)\delta t \\ &\quad + 2\left(Z_{\rm cm}(t) + Dn - d\right)\left(\frac{\beta\omega^2}{2\pi c}\sin(\omega t + \phi)\right)\delta t\,. \end{aligned} \tag{49}$$

The extra terms in δt will reproduce the relativistic contributions provided that

$$\delta t = -\frac{1}{c}\left(Z_{\rm cm}(t) + Dn - d\right), \tag{50}$$

and provided the extra term in ω^2, which arose from the time derivative of the modulation, is negligible. But substituting the solution equation (50) into the last line on equation (49) gives a coefficient that is extremely small:

$$\frac{\beta\omega^2}{\pi c^2} \approx 3 \times 10^{-6}\,. \tag{51}$$

This is a negligible contribution to the fringe count.

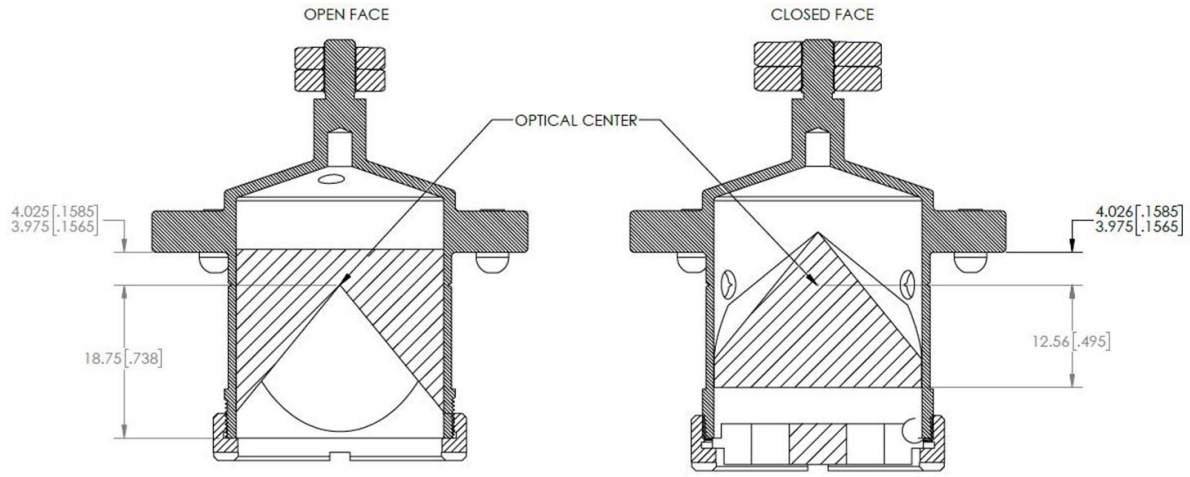

Figure 1 The two test masses used in the experiment. The object on the left has an 'open face' retroreflector (Chamber #2), while the object on the right has the standard 'closed face' retroreflector (Chamber #1). Diagram courtesy of Micro-g LaCoste.

If it were not for modulation terms, the time correction could be expressed as

$$\delta t = \frac{\lambda}{2c}\left(N_{nr}(t) - \frac{\psi}{2\pi}\right) + \frac{1}{2c}(Z_0 + Dn - d)\,, \qquad (52)$$

where $N_{nr}(t)$ is the observed number of fringes at the recorded time t. A similar correction is used in the g9 software.

5. Experimental setup

A Micro-g Lacoste FG5-X absolute gravimeter [9, 10], S/N 302,[6] was operated at the NOAA Table Mountain Geophysical Observatory in August of 2019 [12]. Over the course of three days, two different dropping chambers were installed on the instrument. Chamber #1 is a 'standard' FG5-X dropping chamber, (S/N 102), which employs a solid glass, 'closed face' (n = 1.5) retroreflector. Chamber #2 is a research unit, similar in construction to #1, but with a hollow 'open face' retroreflector comprised of three mirrors. In both chambers, the retroreflectors are housed in a 'test mass' which undergoes free-fall acceleration. Because the center of mass of each test mass needs to be coincident with the optical center of the retroreflector (to minimize second order rotation effects), the test mass of Chamber #2 is necessarily of slightly different construction than that of #1 (figure 1). Otherwise, the dropping chambers are identical: same counter mass design, drop length, nominal vacuum level, etc The rest of FG5X 302's hardware - the laser, interferometer, the seismic isolation device ('Superspring'), the data acquisition hardware, and all cabling - was used in all set ups to minimize any systematic effects between the observations. Before the observations, both chambers were tested to quantify any horizontal velocity of the test mass at the beginning of the drop. Any such motion in the east-west direction will result in a Coriolis acceleration that could systematically and significantly bias the gravity results. However, both chambers registered negligible velocities: Chamber #1 has a Coriolis acceleration equivalent to 0.2 ± 0.1 μGal, and Chamber #2 has no noticeable acceleration at all: 0.0 ± 0.1 μGal. Both values are well within the total uncertainty of the final gravity values, and the 'Coriolis Effect' is henceforth neglected in the analysis.

The first observations employed Chamber #1 and comprised 12 sets of 100 drops at a 5 second drop interval, for a total acquisition time of 12 hours. A second data set with Chamber #1 was then acquired two days later, with a single set of 1000 drops (84 minutes). Next, Chamber #2 was installed, and a set of 500 drops was then acquired (42 minutes). This process was repeated two more times (500 drop sets) for a total of three iterations between the chambers.

Between each setup, care was taken to realign the system to the local plumb line, maximize the interferometer fringe contrast (always between 390 mV and 400 mV, peak-to-peak), and accurately measure the height of the dropping chamber. The g9 software of Micro-g LaCoste was used to process the data, and the default corrections for Earth tide, ocean loading, barometric admittance, and polar motion were applied on a drop by drop basis.

Regardless of which chamber was installed, the drop to drop standard deviation for all runs was between 1.9 and 2.1 μGal. These small values are a strong indication that the object was not significantly rotating in either chamber. Such an effect is usually sporadic, and if it had been present, it would have led to an increased scatter in the results.

6. Experimental results I: applying commercial software

The observation details and gravity results are listed in table 1. Following standard practice in gravimeter cmparisons, the slight difference in the starting heights of the test masses is accounted for by transferring the g value from the actual 'top of the drop,' to a common height of 139.6 cm above the bench

[6] The U. S. Government does not endorse any particular equipment.

Table 1. Experimental Results using commercial software. Height is the distance from the bench mark to the optical center of the retroreflector at the top of the drop. The gravity values are differenced from 979 622 000 μGal. The vertical gravity gradient is used to transfer the raw values to a common height of 139.6 cm above the bench mark.

Dates (2019)	Drop Type	Drops Made(Fit)	Height (cm)	g (μGal)	Std.Dev. (μGal)	Net Uncertainty(μGal)
8.6	solid	1200 (1190)	139.8	710.7	1.6	1.8
8.8	solid	1000 (983)	139.8	709.9	2.0	1.8
8.8	open	500 (484)	139.45	711.3	2.0	1.8
8.9	solid	500 (496)	139.75	710.8	2.0	1.8
8.9	open	500 (488)	139.5	709.9	1.8	1.8
8.9	solid	500 (496)	139.8	710.0	2.2	1.8
8.9	open	500 (494)	139.45	711.4	2.2	1.8

Table 2. Experimental results using commercial software. The mean gravity values are differenced from 979 622 000 μGal. All units are μGal.

Mean Gravity Chamber # 1 (Glass)	710.4
Error of the Mean	1.0
Systematic Uncertainty	0.5
Combined Uncertainty	1.1
Mean Gravity Chamber # 2 (Open)	710.9
Error of the Mean	1.2
Systematic Uncertainty	0.5
Combined Uncertainty	1.3
Difference (Glass-Open)	-0.5
Total Uncertainty	2.4

Table 3. Experimental Results using software based on equation (36). Height is the distance from the bench mark to the optical center of the retroreflector at the top of the drop. The gravity values are differenced from 979 622 000 μGal. The vertical gravity gradient is used to transfer the raw values to a common height of 139.6 cm above the bench mark. Chamber # 1 labels the solid retroreflector.

Date	Chamber	Number of Drops Processed	Height (cm)	Gravity (μGal)	Uncertainty (μGal)
8.6.2019	# 1	1190	139.8	710.3	1.8
8.8.2019	# 1	983	139.8	709.6	1.8
8.8.2019	# 2	485	139.45	711.8	1.8
8.9.2019	# 1	496	139.75	710.7	1.8
8.9.2019	# 2	489	139.5	710.4	1.8
8.9.2019	# 1	496	139.8	709.7	1.8
8.9.2019	# 2	493	139.45	711.9	1.8

mark (an approximate average of the various raw heights) [11]. A vertical gravity gradient of -3.18 μGal cm^{-1} observed at the TMGO Pier, AT, was used to make this transfer. The listed 'uncertainty' is simply the total uncertainty that is reported by the g9 software. As discussed below, it will be reduced when we calculate the difference in gravity observed by the two chambers.

Table 2 lists the mean value of gravity from each dropping chamber, along with the standard deviation of the observations and the standard statistical error. The systematic uncertainty for each measurement is estimated to be 0.5 μGal. This was determined by using the default systematic uncertainty values in the g9 software, but setting the uncertainties of the laser, clock, 'system,' and barometer to zero (as corrections for changes in these effects should be negligible). The 'setup' uncertainty was estimated to be 0.5 μGal (primarily attributed to imperfections in the plumb line alignment and height determination). Next, the statistical uncertainty, $\sigma/\sqrt{N}$, is added in quadrature with the systematic to get a total uncertainty of about 1 μGal for each chamber (compare with the default uncertainty of 1.8 μGal reported in table 1). The final difference in gravity as measured by the two chambers (glass - open) is (-0.5 ± 2.4) μGal, where the final uncertainty on the (correlated) difference is the sum of the combined uncertainties.

7. Experimental results II: new software

The data collected by dropping both solid and open retroreflectors, described in section 5, was also processed using software based on the relativistic treatment using equation (36), above. Frequency modulation of the interference signal is represented by including the constants A and B, as derived in section 3; this modulation theory includes both non-relativistic and relativistic effects arising from the last factor in equation (36). Frequency modulation coefficients suggested in [9] would be equivalent to the replacement

$$\left(A\cos(\omega t) + B\sin(\omega t)\right)\left(F_{nr} + \frac{1}{c}F_{\rm rel}\right) \to A\cos(\omega t) + B\sin(\omega t)\,. \tag{53}$$

The present model was derived in section 3; rms residuals are approximately 0.0024 fringes and are a few percent smaller than the replacement modulation scheme suggested in equation (53) .

The data for each of the solid/open retroreflectors was processed in two ways. One way consisted of combining both non-relativistic and relativistic effects, as expressed in equation (36). With this model the non-relativistic effects can be separated out by taking $c \to \infty$; fitting with this

Table 4. Experimental results using software based on equation (36). The mean gravity values are differenced from 979 622 000 μGal. All units are μGal.

Mean Gravity Chamber # 1 (Glass)	710.1
Error of the Mean	1.1
Systematic Uncertainty	0.5
Combined Uncertainty	1.2
Mean Gravity Chamber # 2 (Open)	711.4
Error of the Mean	1.2
Systematic Uncertainty	0.5
Combined Uncertainty	1.3
Difference (Glass-Open)	-1.3
Total Uncertainty	2.4

completely non-relativistic model, the relativistic corrections can be calculated using equation (45). The differences between the fully relativistic model and the non-relativistic model for g_t were found to be equal to the relativistic corrections to within 0.01 μGal. In all cases the relativistic corrections were −13.9 μGal so a separate column for these corrections is not given in table 3. The results for the complete model including relativistic effects are given in table 4.

8. Conclusions

Comparison of the values of gravity determined by dropping open and solid glass retroreflectors shows good agreement, to within the estimated uncertainties. Statistical and systematic uncertainties are dependent on the gravimeter used for the measurements and are the same for retroreflectors of both types. Although no valid error has been found in the expression in [1] for the phase difference between interference and test beams when combined at the beamsplitter, literal application of that difference to experimental data leads [1] to a prediction of several μGal difference in g between open and solid retroreflectors; this difference disappears when the ambiguity in the argument of a trigonometric function such as a cosine is accounted for. The intensity of the interference fringe pattern contains constant terms:

$$|\Psi|^2 \approx \cos\left(-\frac{2}{\lambda}(Z_0 + Dn - d) + \ldots.\right). \tag{54}$$

Whether open or solid, such terms cannot be measured because a constant $2\pi M$, where M is an arbitrary integer, can be added to the argument of the cosine reducing the argument to a polynomial in the time with negligible constant terms.

An improved treatment of the effect of frequency modulation, with modulation index $\beta >> 1$ has been given, implemented in software, and applied to data for both open and solid retroreflectors. Typically for a given drop with a time series of more than 2400 times, each corresponding to a fringe spacing of 400 fringes, the rms residual between the specified number of fringes and the theoretical number, given by equation (36), is 0.02 fringes. Two methods for computing relativistic corrections have been implemented: (1) the difference between gravity determined by the fully relativistic model, and (2) the matrix calculation given by equation (45). These two methods consistently give -13.88 μGal for relativistic corrections in the present case.

Appendix: Distance of fall vs. wavelength

The phase difference between reference and test beams if recombined at the beamsplitter is given in equation (2). The corresponding number of fringes is obtained by replacing Ω by $2\pi c/\lambda$ and dividing by 2π. The number of fringes is then

$$N(t) = -\frac{2}{\lambda}(Z_{\rm cm}(t) + Dn - d)\left(1 - \frac{V_{\rm cm}(t)}{c}\right) + \text{constant}. \tag{A1}$$

Suppose that during some small time interval the CM position and velocity change by $\Delta Z_{\rm cm}$ and $\Delta V_{\rm cm}$, respectively. The number of fringes observed will be

$$\Delta N = -\frac{2}{\lambda}(\Delta Z_{\rm cm})\left(\left(1 - \frac{V_{\rm cm}(t)}{c}\right) + \frac{2}{\lambda}(Z_{\rm cm}(t) + Dn - d)\left(\frac{\Delta V_{\rm cm}(t)}{c}\right)\right). \tag{A2}$$

If the retroreflector falls by a half-wavelength, $\Delta Z_{\rm cm} = -\lambda/2$, then the number of fringes observed will be

$$\Delta N = 1 - \frac{V_{\rm cm}(t)}{c} + \frac{2}{c\lambda}(Z_{\rm cm}(t) + Dn - d)\Delta V_{\rm cm}(t). \tag{A3}$$

and the number is unity, with relativistic corrections.

ORCID iD

Neil Ashby https://orcid.org/0000-0003-0719-3979

References

[1] Ashby N 2017 Relativistic theory of the falling retroreflector gravimeter *Metrologia* **55** 1–19
[2] Kren P and Palinkas V *Metrologia* 55 2018 314–15
[3] Nagornyi V D 2018 *Metrologia* **55** 446–7
[4] Svitlov S 2018 *Metrologia* **55** 605–13
[5] Ashby N 2018 *Metrologia* **55** 316–17
[6] Ashby N 2018 *Metrologia* **55** 448–9
[7] Ashby N 2018 *Metrologia* **55** 614–17
[8] D'Agostino G 2019 *Metrologia* **56** 052101
[9] Niebauer T M, Sasagawa G S, Faller J E, Hilt R and Klopping F 1995 *Metrologia* **32** 159–80
[10] Niebauer T M, Billson R, Schiel A, van Westrum D and Klopping F 2013 The self-attraction correction for the FG5X absolute gravity meter *Metrologia* **50** 1–8
[11] Wu S, Feng J and Li C *et al* 2019 The results of CCM.G-K2.2017 key comparison *Metrologia* **57** 07002–07002 (https://www.bipm.org,/utils/common/pdf/finalreports/M/G-K2/CCM.G-K2.2017.pdf)
[12] van Westrum D 2020 North American Regional Comparison of Absolute Gravimeters (NACAG18) NOAA Technical Memorandum NOS NGS 80) National Geodetic Survey, Silver Spring, MD USA
[13] Wallard A 1972 *J. Phys. E. Sci. Instrum* **5** 926